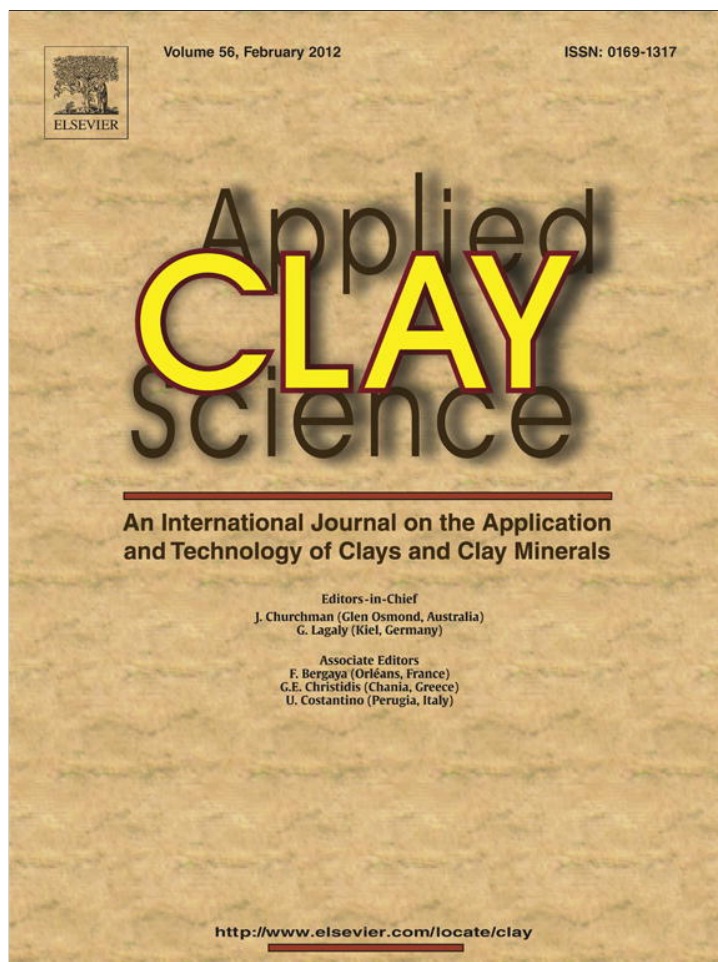


Provided for non-commercial research and education use.  
Not for reproduction, distribution or commercial use.



This article appeared in a journal published by Elsevier. The attached copy is furnished to the author for internal non-commercial research and education use, including for instruction at the authors institution and sharing with colleagues.

Other uses, including reproduction and distribution, or selling or licensing copies, or posting to personal, institutional or third party websites are prohibited.

In most cases authors are permitted to post their version of the article (e.g. in Word or Tex form) to their personal website or institutional repository. Authors requiring further information regarding Elsevier's archiving and manuscript policies are encouraged to visit:

<http://www.elsevier.com/copyright>



## Research paper

## Synthesis and adsorption characteristics of hollow spherical allophane nano-particles

Fumitoshi Iyoda <sup>a</sup>, Shuhei Hayashi <sup>a</sup>, Shuichi Arakawa <sup>a</sup>, Baiju John <sup>a</sup>, Masami Okamoto <sup>a,\*</sup>,  
Hidetomo Hayashi <sup>b</sup>, Guodong Yuan <sup>c</sup>

<sup>a</sup> Advanced Polymeric Nanostructured Materials Engineering, Graduate School of Engineering, Toyota Technological Institute, 2-12-1 Hisakata, Tempaku, Nagoya 468 8511, Japan

<sup>b</sup> New Product Development Center, Tsuchiya Co., Ltd., 22-4 Higashinamikita, Yamamachi, Chiryu, 472-0006, Japan

<sup>c</sup> Landcare Research, Private Bag 11052, Palmerston North 4442, New Zealand

## ARTICLE INFO

## Article history:

Received 4 June 2011

Received in revised form 25 November 2011

Accepted 25 November 2011

Available online 20 December 2011

## Keywords:

Allophanes

Nanoparticles

Adenine

5'-AMP

Adsorption

## ABSTRACT

We synthesized three allophanes from precursors by a hydrothermal reaction at 100 °C for 48 h. The precursors were formed from the solutions of Na<sub>4</sub>SiO<sub>4</sub> and AlCl<sub>3</sub>·6H<sub>2</sub>O at different Si/Al molar ratios (0.5, 0.75, 1.0). The nanostructure of the synthetic allophanes was compared with that of a natural allophane from New Zealand by using X-ray diffractometry, energy dispersive X-ray spectroscopy, Fourier-transform infrared spectroscopy, thermogravimetry/differential thermal analysis, <sup>29</sup>Si and <sup>27</sup>Al magic angle spinning (MAS) nuclear magnetic resonance (NMR), field emission electron microscopy, and pore-size distribution based on the Cranston–Inkley method. The propensity of the allophanes to adsorb adenine and adenosine-5'-monophosphate (5'-AMP) was assessed by batch experiments. The adsorption data were fitted by the Freundlich equation and the adsorption parameters were discussed in relation to the properties of the natural and synthetic allophanes. The adsorption capacity (*K<sub>f</sub>*) of the natural allophane for 5'-AMP was three times that for adenine. The average *K<sub>f</sub>* value of the three synthetic allophanes for 5'-AMP was more than twice that of the natural allophane, possibly due to the higher purity of the synthetic allophanes.

© 2011 Elsevier B.V. All rights reserved.

## 1. Introduction

In many parts of the world water bodies are becoming increasingly contaminated by compounds from a wide range of human activities such as agriculture, manufacturing, energy consumption, and waste disposal. A report from the World Health Organization (WHO) shows that at least 1.1 billion people in the world lack access to improved/safe water sources and more than 2.6 billion are without basic sanitation (WHO, 2007). Thus, there is an increasing demand on research for cost-effective materials and technologies for water treatment.

Particle size and surface area are important features of adsorbent materials for use in water treatment to remove toxic and carcinogenic contaminants (Theng and Yuan, 2008). A small particle size, a large specific surface area, and surface functional groups of materials are often desirable for their better adsorption of extraneous contaminants (Yuan and Wada, 2012). In this regard, allophane is the nanomaterial of choice for environmental applications because of its ability of adsorbing cations (e.g., Cu<sup>2+</sup>), anions (e.g., phosphate and arsenate), and organic molecules. Allophane is a short-range-order clay mineral and occurs in some soils derived from volcanic ejecta. The primary particles of the allophane are hollow spherules with an outer diameter of 3.5–5.0 nm and a perforated wall about 0.6–1.0 nm thick (Brigatti et al., 2006 and references therein). The specific surface area of allophane is as high as ~900 m<sup>2</sup>/g, which is often larger than that of activated

carbon. Further, the (OH)Al(OH<sub>2</sub>) groups exposed on the wall perforations are the source of the pH-dependent charge characteristics of allophane. They become <sup>+</sup>(OH<sub>2</sub>)Al(OH<sub>2</sub>) by acquiring protons on the acid side of the point of zero charge, and become (OH)Al(OH)<sup>-</sup> by losing protons on the alkaline side. Finally, the groups can form inner-sphere complexes with the carboxylic groups of organic compounds (Yuan and Wada, 2012).

Allophane content in volcanic soils is variable, usually much lower than the upper limit of 35–40%. In other words, natural allophane contains undesirable impurities like sand, silt, and clay-size particles that are difficult to be separated. Thus, naturally derived pure allophane with consistent compositions and properties is not commercially available. Rather, natural allophane has a variable composition: its Si/Al molar ratio changes with the environment (Parfitt, 1990) and is typically between 0.5 and 1. In this report, three synthetic allophanes with different Si/Al ratios were prepared and characterized. The adsorption properties were assessed against a natural allophane, using adenine and adenosine 5'-monophosphate (5'-AMP) as adsorbates. 5'-AMP is a nucleotide and adenine plays an important role in biological systems.

## 2. Materials and methods

## 2.1. Allophanes

A New Zealand allophane (NP76) sample was obtained by the dispersion of a subsoil sample (from New Plymouth in the North Island) in water at pH 3.5 by ultrasonication, sedimentation under gravity,

\* Corresponding author. Tel.: +81 52 809 1861; fax: +81 52 809 1864.  
E-mail address: [okamoto@toyota-ti.ac.jp](mailto:okamoto@toyota-ti.ac.jp) (M. Okamoto).

separation of the <2  $\mu\text{m}$  fraction, coagulation with 1 M NaCl at pH ~6.5, and dialysis against deionized water until free of chloride. The Si/Al ratio of the sample was determined by dissolution in acidic ammonium oxalate solution (Theng et al., 1982).

The precursor gels (Si/Al ratio = 0.50, 0.75 and 1.00) for the allophane synthesis were prepared by mixing and stirring (for 1 h) of 100 mM of sodium silicate, ortho ( $\text{NaSiO}_4$ , Nacalai-Tesque) and aluminum chloride hexahydrate ( $\text{AlCl}_3 \cdot 6\text{H}_2\text{O}$ , Sigma-Aldrich). The sodium chloride formed was removed by centrifugation at a speed of 5000 rpm for 5 min. The precursors were then autoclaved at 100 °C for 48 h (Ohashi et al., 2002). The high feed concentration was necessary for a high yield of allophane that would be suitable for the synthesis on an industrial scale.

The synthesized samples were designated as 100Si/Al-x (x: Si/Al ratio; for e.g., 100Si/Al-1.0) and 'Pre-' refers to the precursors.

## 2.2. Characterization

The crystal structure of allophanes was characterized by wide-angle X-ray diffraction (WAXD) (Mxlabo, MAC Science Co.,  $\text{CuK}\alpha$  radiation, wavelength  $\lambda = 0.154$  nm), and structural changes were determined by Fourier-transform infrared (FTIR) spectra collected at a resolution of  $2\text{ cm}^{-1}$  using a FTIR spectrometer (FT-730, Horiba Ltd). The morphological features of the allophanes were observed by field emission scanning electron microscopy (FE-SEM) (S-4700, Hitachi Ltd) equipped with elemental analysis by energy dispersive X-ray spectroscopy (EDX) (EMAX-7000, Horiba Ltd) after the samples were sputter-coated with platinum under an argon pressure of 10 Pa for 1 min at a current of 10 mA.

The chemical and structural surroundings of both Si and Al ions were measured using  $^{27}\text{Al}$  and  $^{29}\text{Si}$  magic angle spinning (MAS) solid-state nuclear magnetic resonance (NMR). The  $^{27}\text{Al}$  and  $^{29}\text{Si}$  solid-state MAS NMR spectra were collected with a Varian Unity INOVA 400 spectrometer (9.4 T) equipped with 4-mm and 7.5-mm chemagnetics double-resonance MAS probes, respectively. The resonance frequency at this magnetic field was 104.19 MHz for  $^{27}\text{Al}$  and 79.44 MHz for  $^{29}\text{Si}$ .

For  $^{27}\text{Al}$  MAS NMR measurement, the spectra were taken after  $\pi/2$  pulse irradiation (1.1  $\mu\text{s}$  as a pulse width) with a recycle time of 1 s. The number of transients was selected as 1024 in order to improve the signal/noise ratio and the samples were spun at 10 kHz. For  $^{29}\text{Si}$  MAS NMR measurement,  $\pi/2$  pulse irradiation (4.0  $\mu\text{s}$  as a pulse width) was also used. The recycle time, the number of transients, and the sample spinning rate were 10 s, 4096, and 5 kHz. The chemical shifts for  $^{27}\text{Al}$  and  $^{29}\text{Si}$  were referenced to the positions of  $[\text{Al}(\text{H}_2\text{O})_6]^{3+}$  of 1 M  $\text{Al}(\text{NO}_3)_3$  aqueous solution and tetramethylsilane (TMS).

The thermal behavior was determined by thermogravimetry/differential thermal analysis (TG/DTA 6300, Seiko Instruments Inc.) at a heating rate of 5 °C/min under air with a flow rate of 260 ml/min.

The pore volume and pore size distribution were measured by the Cranston-Inkley (CI) method (Cranston and Inkley, 1957) using a nitrogen adsorption-desorption approach (BELSORP-mini, Bel Japan, Inc.). The specific surface area was estimated by the *t*-method (Lippens and de Boer, 1965).

## 2.3. Adsorption experiments

Adenine was purchased from Kanto Chemicals, Japan, and 5'-AMP from Wako Pure Chemicals, Japan. 10 mg of a synthetic allophane, natural allophane, or a precursor gel was dispersed in 10 ml of 0.1–2.0 mM aqueous solutions of adenine or 5'-AMP and shaken for 60 h at room temperature. The dispersions were then centrifuged at 5000 rpm for 10 min. The total organic carbon (TOC) and total nitrogen (TN) in the supernatants were measured by an Analytik Jena

multi N/C 2100S instrument, using the combustion method at 800 °C after four-point calibration.

## 2.4. Molecular modeling of adsorbates

Using a molecular dynamics program (MM3 Scigress, ver.2.1, Fujitsu Ltd.), we proposed the molecular dimensions of adenine and 5'-AMP by taking their van der Waals radii into account. Optimization of the molecular structure was based on the minimization of the total energy of the molecular system.

## 3. Results and discussion

### 3.1. Morphological features

Based on the morphology of the allophane samples, Fig. 1 shows the probable structure of the spherule wall, the wall perforations, and the intra-spherule void. The overall size of a single allophane particle is ~5 nm. The functional groups  $(\text{HO})\text{Al}(\text{OH}_2)$  exposed on the wall perforations play a significant role in the adsorption processes.

The nitrogen adsorption-desorption isotherms of two synthetic allophanes (Fig. 2) were type IV isotherms with some hysteresis loops indicating mesopores (Mohanani et al., 2005). For 100 Si/Al-1.0, the loop area and the amount of adsorbed nitrogen were less than those of 100 Si/Al-0.5.

The pore-size distribution of natural and synthetic allophanes and precursor showed a peak at ~1.9 nm (Fig. 3). Natural allophane (NP76) and synthetic allophane (100Si/Al-0.5) had a similar Si/Al ratio but different pore sizes and volumes. The larger specific pore volume of 100Si/Al-0.5 compared to 100Si/Al-1.0 (Table 1) was presumably due to the contribution of the pore radius ( $R_p$ ) in the range of ~3.0 nm (Fig. 3). For the allophanes, but not for the precursors, the appearance of a peak at ~1.9 nm was a common feature.

The FE-SEM image of NP76 clearly shows the spherical nature of allophane observed (Fig. 4a). The high resolution image of transmission electron microscope (Yuan and Wada, 2012) showed clustered or agglomerated particles, rather than singular particles. Removal of the humic substances from this natural allophane by 10%  $\text{H}_2\text{O}_2$  at 100 °C for 12 h (Hashizume and Theng, 2007) resulted in the disintegration of the bulk into smaller aggregates (Fig. 4c). The EDX spectrum of NP76 (Fig. 4(d)) confirmed the presence of impurities such as Fe-containing minerals, which also appeared in the spectrum of  $\text{H}_2\text{O}_2$ -treated allophane (image not shown).

The average value of the particle size, was estimated from the SEM images (Fig. 5) as described by Sinha et al. (2003). The particle size of synthetic allophanes increased from  $18.0 \pm 3.8$  to  $22.9 \pm 4.2$  nm with

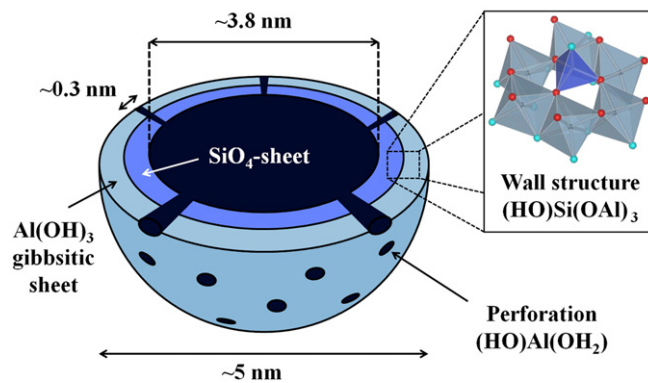


Fig. 1. Schematic representation of allophane structure.

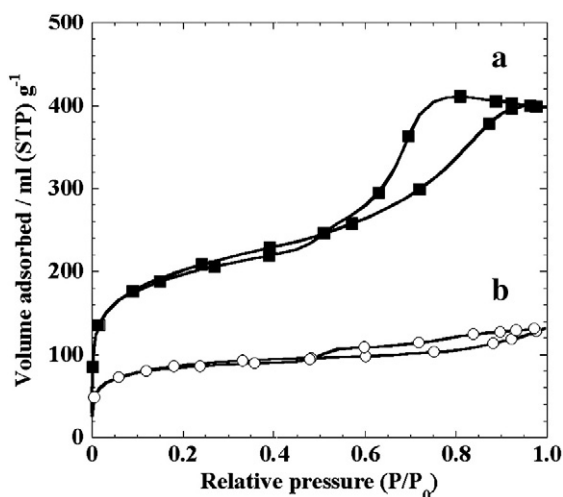


Fig. 2. Nitrogen adsorption–desorption isotherms of synthetic allophanes: (a) 100Si/Al-0.5; (b) 100Si/Al-1.0.

increasing Si/Al ratio due to the increased amount of Si in the inner sheet of the particles. The average particle size was much larger than that of the primary particles of allophane because of aggregation. The size of the precursor, *Pre*-100Si/Al-0.5 without pores (Fig. 5c), was much larger than that of the corresponding synthetic allophane.

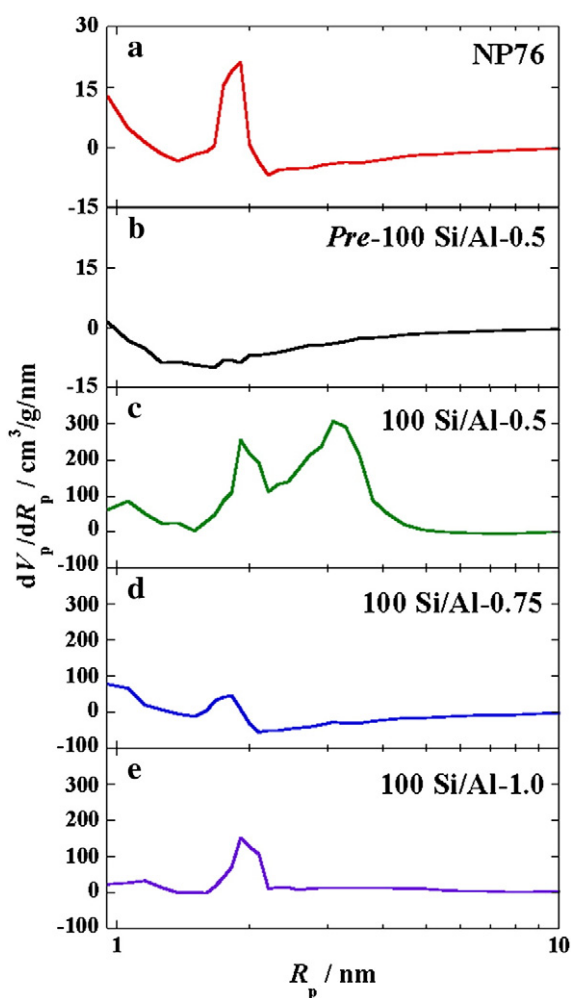


Fig. 3. Pore-size distributions of (a) NP76; (b) *Pre*-100Si/Al-0.5; (c) 100Si/Al-0.5; (d) 100Si/Al-0.75; (e) 100Si/Al-1.0.

The reason is presently not obvious. However, the precursor showed a spherical morphology. As revealed by  $^{27}\text{Al}$  and  $^{29}\text{Si}$  MAS NMR analyses (Fig. 9), the hydrothermal reaction densified the structure of the precursor particles.

### 3.2. Structural changes

Fig. 6 shows the characteristic FTIR spectra of NP76 and synthetic allophanes in the region of  $1800\text{--}400\text{ cm}^{-1}$ . A band located at  $3450\text{ cm}^{-1}$  (data not shown) was assigned to the structural OH stretching mode, ( $\nu(\text{OH})$ ), and the band at  $1645\text{ cm}^{-1}$  was due to the hydroxyl bending vibration ( $\delta(\text{OH}_2)$ ) from absorbed water. The characteristic bands were observed in the range of  $1200\text{--}800\text{ cm}^{-1}$  (stretching mode:  $\nu(\text{Si-O})$  and/or  $\nu(\text{Al-O})$ ) and  $800\text{--}400\text{ cm}^{-1}$  ( $\nu(\text{Si-O-Si})$  and/or  $\nu(\text{Al-O-Si})$ ). The bands at  $1025\text{ cm}^{-1}$  and  $974\text{ cm}^{-1}$  were characteristic of gibbsite, showing an increased gibbsite formation with increasing Si/Al ratio (Loyghnan, 1969). The presence of well-ordered gibbsite in 100Si/Al-0.5 was also confirmed. The intensity ratio of [ $\nu(\text{Si-O})$  and/or  $\nu(\text{Al-O})$ ]/[ $\nu(\text{Si-O-Si})$  and/or  $\nu(\text{Al-O-Si})$ ] increased with the Si/Al ratio in the parent solutions. This trend adversely affected the formation of gibbsite. The bands at  $670$  and  $430\text{ cm}^{-1}$  originated from the peculiar wall structure of allophane ((HO)Si(OAl) $_3$ ) (Parfitt, 1990). The FTIR spectra of  $\text{H}_2\text{O}_2\text{NP76}$  and NP76 with similar bands imply that the removal of humic substances did not affect the internal structure of the natural allophane.

The WAXD patterns of NP76 and synthetic allophanes showed a broad reflection at  $2\theta \sim 26^\circ$  ( $0.34\text{ nm}$ ) and  $\sim 40^\circ$  ( $0.23\text{ nm}$ ), indicating the amorphous nature. However, a small shoulder at  $2\theta = 6\text{--}12^\circ$  ( $0.74\text{--}1.5\text{ nm}$ ) suggested the short-range order of allophanes (Van der Gaast et al., 1985). Thus, allophanes are more appropriately defined as nanosized, short-range ordered aluminosilicates (Fig. 7).

The strong 002, 200, and 312 reflections at  $2\theta = 18.18^\circ$ ,  $20.18^\circ$  and  $40.48^\circ$  were assigned to gibbsite. The enhanced formation of a gibbsite phase at a high ratio of Al (Si/Al = 0.5) was accompanied by the appearance of three different pore radii ( $1.06$ ,  $1.91$  and  $3.09\text{ nm}$ ) (Fig. 3).

The sharp reflections observed in NP76 were due to the Fe-containing impurities, as also confirmed by the EDX data (Fig. 4d). This natural allophane might have a significant structural variation due to irregularities in the pore structure.

The TGA curves of  $\text{H}_2\text{O}_2\text{NP76}$  indicated a 5% decrease in mass compared with NP76 due to the removal of the humic substance by  $\text{H}_2\text{O}_2$  (Fig. 8). The natural and synthetic allophanes showed similar TG thermograms. They lost absorbed water between  $50$  and  $110^\circ\text{C}$ . 100Si/Al-0.5 exhibited a significant mass loss at around  $250^\circ\text{C}$ , accompanied by a corresponding endothermic peak which was due to the dehydration and decomposition of gibbsite. The natural allophane showed a much lower mass loss at  $500^\circ\text{C}$ . Its thermal stability was much better than that of the synthetic allophanes, presumably due to the various cationic impurities in the balance of spherule structure.

Fig. 9 shows  $^{27}\text{Al}$  and  $^{29}\text{Si}$  MAS NMR spectra of allophanes. The peak at  $-78\text{ ppm}$  of the  $^{29}\text{Si}$  spectrum corresponds to the wall structure ((HO)Si(OAl) $_3$ ) consisting of Si tetrahedra attached to three aluminol groups (Al-OH) of the gibbsite sheet and one silanol group (( $Q^3$ )Al) by Engelhardt (1996). In the notation  $Q^n$ , where  $Q$  is the Si atom bound to four O atoms with a tetrahedral structure and  $n$  indicates the connectivity. No significant peak shift at  $-78\text{ ppm}$  was observed for all precursors and synthetic allophanes. There was a broad resonance between  $-83$  and  $-89\text{ ppm}$ . This peak may suggest that the different chemical structure surroundings of the Si atoms shift the resonance to higher or lower values with the number of Al atoms bound to the central Si atom.

With increasing Si/Al ratio, the broad peak around  $-85\text{ ppm}$  shifted towards a lower value. This trend was more obvious for the precursors than for the corresponding synthetic allophanes,

**Table 1**  
Properties of natural and synthetic allophanes.

Samples	Particle size/nm	Molar Si/Al <sup>a</sup> ratio	Pore size <sup>b</sup> 2R <sub>p</sub> /nm	Pore specific volume/mm <sup>3</sup> /g	Specific surface area/m <sup>2</sup> /g
NP76	–	0.53	3.82	–	~900 <sup>c</sup>
100 Si/Al-0.5	18.0 ± 3.8	0.56	2.12, 3.82, 6.18	464	700
100 Si/Al-0.75	20.6 ± 4.2	0.82	3.64	–	–
100 Si/Al-1.0	22.9 ± 4.2	1.07	3.80	109	630
Pre-100 Si/Al-0.5	21.3 ± 5.2	0.63	nil	–	–

<sup>a</sup> Calculated by EDX except for NP76 (calculated from acid ammonium oxalate extractable Al and Si contents).

<sup>b</sup> Estimated by the CI method.

<sup>c</sup> Hashizume and Theng (2007).

indicating that allophanes were structurally more stable than precursors. In this study, a clear explanation could not be obtained. However, the major chemical shifts of Q<sup>3</sup>1<sup>vi</sup>Al (–84 to –91 ppm) and Q<sup>3</sup>2<sup>vi</sup>Al (–81 to –86 ppm) (Engelhardt, 1996) were due to the formations on the convex surface of the spherule wall of allophanes with Si/Al ratio.

In the case of NP76, the resonance at –93 ppm was related to the impurities, as suggested by Hiradate (2004). These impurities included volcanic glasses and silica gels.

In the <sup>27</sup>Al NMR spectra, the 5 ppm peak indicates Al atoms with octahedral coordination (<sup>vi</sup>Al) while the peak at 60 ppm corresponds to tetrahedrally coordinated Al atoms (<sup>iv</sup>Al) (Hiradate and Wada, 2005). The <sup>iv</sup>Al atoms were substituting the Si atoms of the outer-sheet and represent the octahedral gibbsite layer. A weak peak at 35 ppm in the spectra of the precursors indicated fivefold coordinate Al atoms of the disordered structures. Due to the structural transformations of the precursor into the allophane formation, both <sup>iv</sup> and <sup>v</sup> Al atoms disappeared. The reduction of the Si/Al ratio (from 1.0 to 0.5) exhibited a decrease in the integral intensity (*I*<sub>(iv)</sub>/*I*<sub>(vi)</sub>) of the synthetic allophanes due to the formation of octahedral gibbsite layers (Fig. 10).

### 3.3. Adsorption properties

The adsorption isotherms of adenine and 5'-AMP on natural and synthetic allophanes (Fig. 11) were fitted by the Freundlich equation ( $r^2 \geq 0.90$ ),

$$Q_{\text{ads}} = K_f [A]_e^{1/N} \quad (1)$$

where  $K_f$  is the relative adsorption capacity of the adsorbent and  $N$  is the adsorption intensity, which describes the shape of the isotherm (Table 2). The adsorption isotherms exhibited a marked curvature, with slopes ( $1/N$ ) significantly < 1.0, indicating a convex curvature or *L*-type isotherm. The slope of the isotherms decreased with increasing adsorptive concentration because the vacant sites became less accessible with progressive covering of the adsorbent surface (Giles et al., 1960).

The adsorption of 5'-AMP by NP76 showed a much larger value of  $K_f$  (0.18) than that of adenine. The removal of humic substances by H<sub>2</sub>O<sub>2</sub> slightly increased the  $K_f$ . The humic substances and the metallic impurities of NP76 significantly reduced the adsorption in

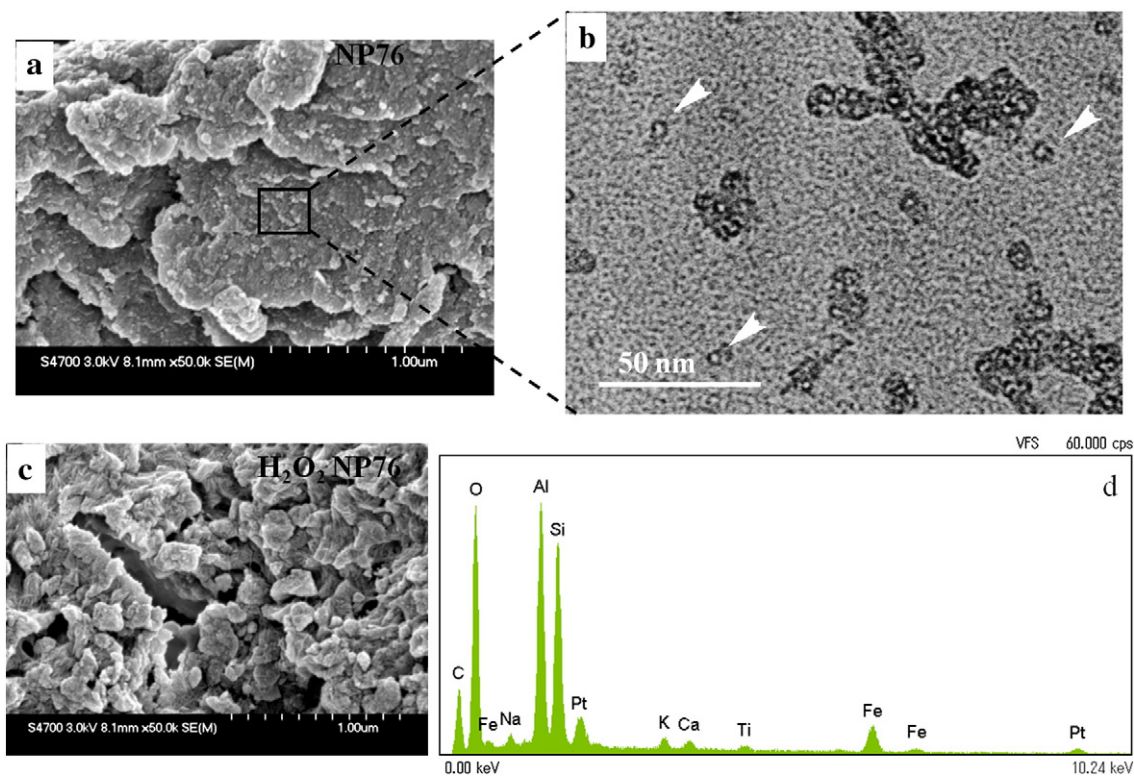


**Fig. 4.** (a) FE-SEM image of (a) NP76, (b) the magnified HR-TEM image of the inset region, (c) FE-SEM image of H<sub>2</sub>O<sub>2</sub> reacted NP76 and (d) EDX spectra of NP76. The arrows indicate the unit particle of aluminosilicate allophane with an outer diameter of 3.5–5.0 nm.

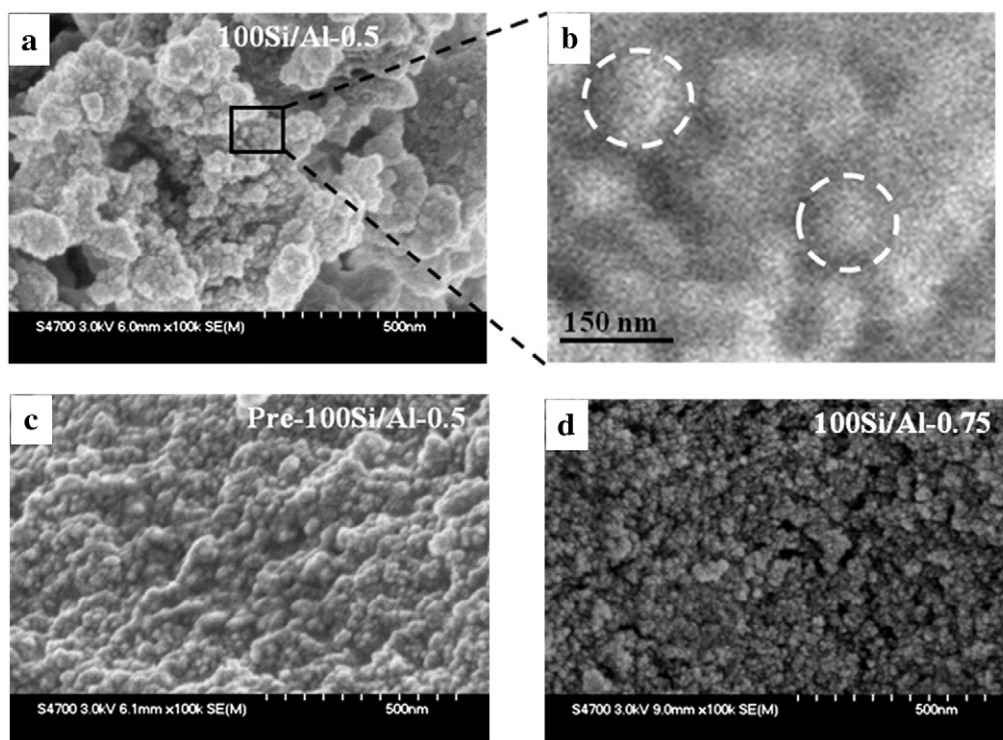


Fig. 5. FE-SEM images of synthetic allophanes: (a) 100Si/Al-0.5; (b) magnified image of the inset region; (c) precursor of 100Si/Al-0.5; (d) 100Si/Al-0.75.

comparison with synthetic allophanes. The absence of pores might have contributed to the low  $K_f$  value of the precursor.

Because of the incompatible dimensions of the wall perforations (~0.3 nm) of allophane and the size of adenine and 5'-AMP (Fig. 12), the adsorptives could not enter the internal cavity of allophane. Thus, the SiOH groups on the internal surface of allophane did not contribute to the adsorption of adenine and 5'-AMP. However, the allophane spherules existed as aggregates and not as single particles. The interstitial space between the spherules could accommodate adenine and 5'-AMP molecules. Electrostatic, hydrogen bonding and van der Waals interactions also contributed to the adsorption of these molecules.

Analysis of the adenine and 5'-AMP adsorption isotherms suggest that the adsorbed molecules likely form monolayers. The larger  $K_f$  value for 5'-AMP (Table 2) compared to adenine suggests a superior adsorption. The adsorption of 5'-AMP was facilitated by the interaction

of the phosphate groups with the Al–OH groups on the wall perforations, involving the formation of inner-sphere complexes through a ligand-exchange reaction between Al–OH and  $(\text{HO})_2\text{OP}=\text{O}$  groups (Hashizume and Theng, 2007).

#### 4. Conclusions

Three allophanes with Si/Al molar ratios of 0.5, 0.75 and 1.0 were synthesized and compared with a natural allophane sample. The natural and synthetic allophanes were poorly crystalline and consisted of hollow spherules of ~3.8 nm internal diameter and a characteristic wall structure composed of  $(\text{HO})\text{Si}(\text{OAl})_3$  groups. The adsorption of 5'-AMP ( $K_f$ ) on the natural allophane sample was three times higher compared to adenine. The strong adsorption of 5'-AMP by allophane may be due to the formation of inner-sphere complexes between the

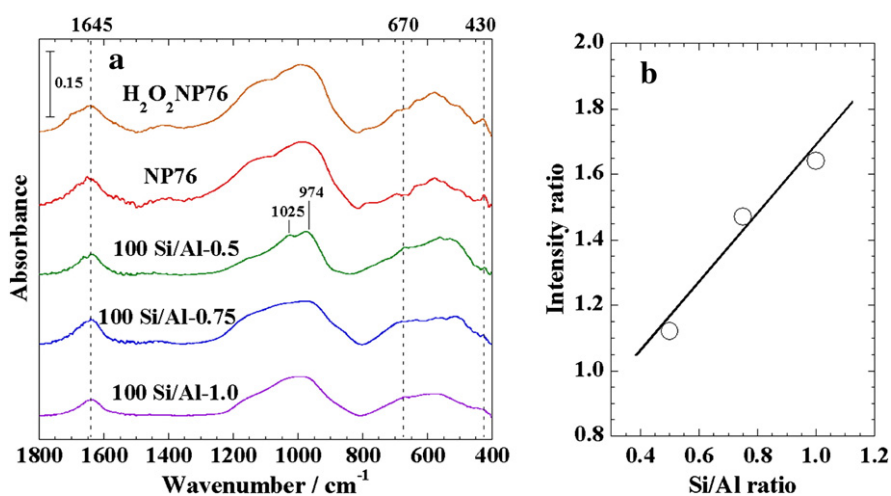


Fig. 6. (a) FT-IR spectra of natural and synthetic allophanes in the region of 1800–400  $\text{cm}^{-1}$ . Data on the Y-axis were shifted to avoid overlapping. (b) intensity ratio of  $[\nu(\text{Si}-\text{O}) \text{ and/or } \nu(\text{Al}-\text{O})]/[\nu(\text{Si}-\text{O}-\text{Si}) \text{ and/or } \nu(\text{Al}-\text{O}-\text{Si})]$  versus Si/Al ratio.

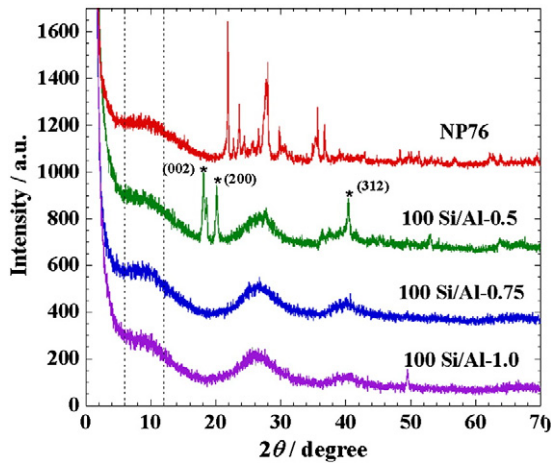


Fig. 7. WAXD profiles of natural and synthetic allophanes. The data on Y-axis were shifted to avoid overlapping. The dashed lines indicate the position of the remnant shoulder. The asterisks indicate the strong reflections of gibbsite.

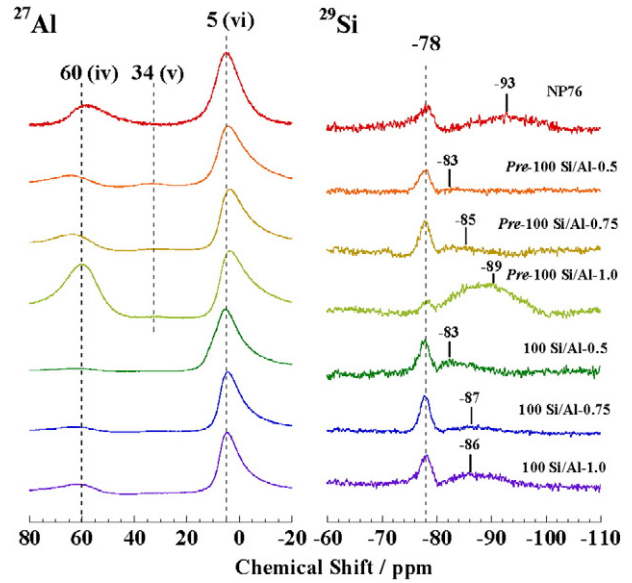


Fig. 9. <sup>27</sup>Al and <sup>29</sup>Si MAS solid-state NMR spectra of natural and synthetic allophanes.

Al–OH and (HO)<sub>2</sub>OP=O groups. The average *K<sub>f</sub>* value (0.39) for the 5'-AMP adsorption on the synthetic allophanes was distinctly higher than for the natural allophane (0.18). This may be explained by the higher purity of the synthetic allophanes. The influence of the Si/Al ratio on the adsorption of 5'-AMP by the synthetic allophanes was not consistent. In the applications side, the possibility of using alternating layers of natural and synthetic allophanes in a filter system for water purification may be considered for a better cost-effectiveness.

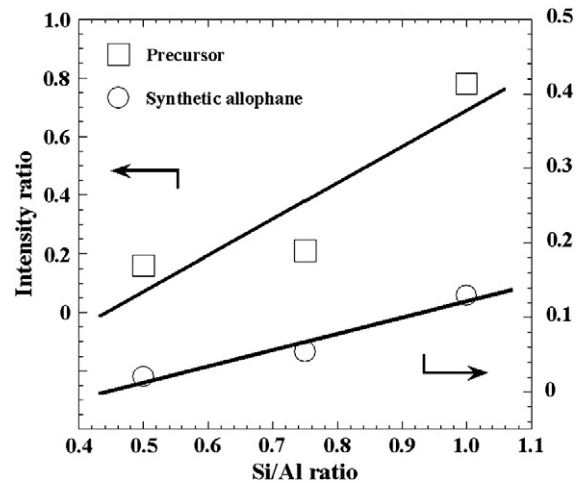


Fig. 10. Integral intensity ratio of (*I*<sub>(iv)</sub>/*I*<sub>(vi)</sub>) for <sup>27</sup>Al spectra versus Si/Al atomic ratio. (The solid lines are for visual help.)

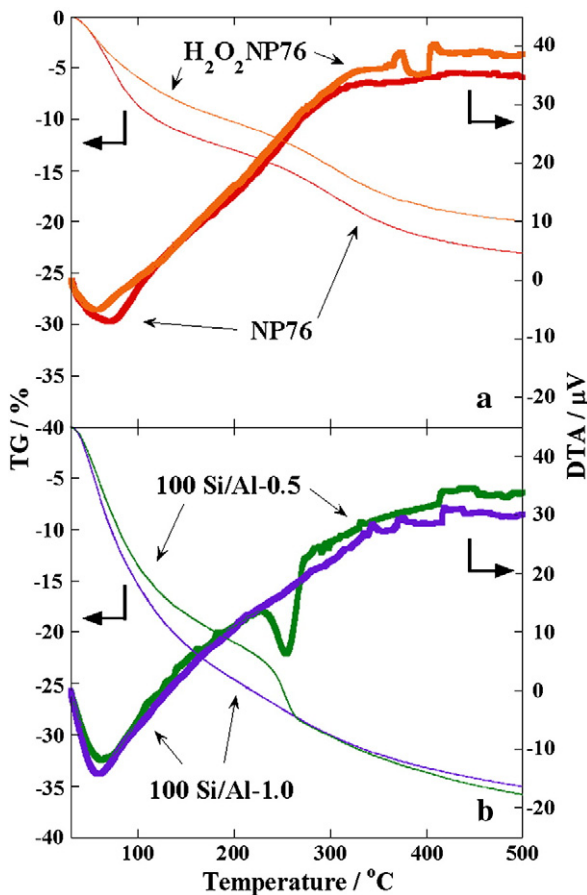


Fig. 8. TGA/DTA curves of (a) NP76 and H<sub>2</sub>O<sub>2</sub>NP76; (b) synthetic allophanes of 100Si/Al-0.5 and 100Si/Al-1.0.

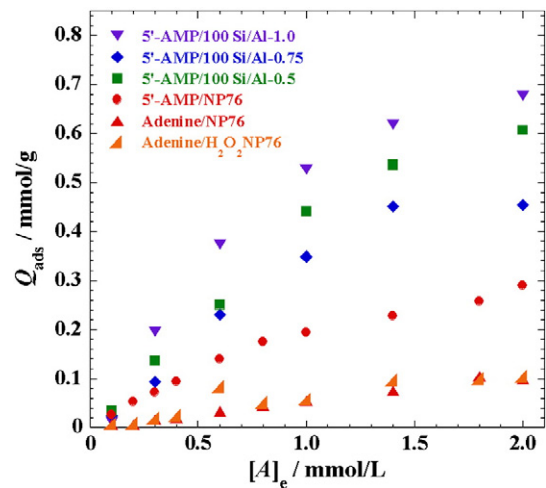


Fig. 11. Adsorption isotherms of adenine and 5'-AMP on natural and synthetic allophanes.

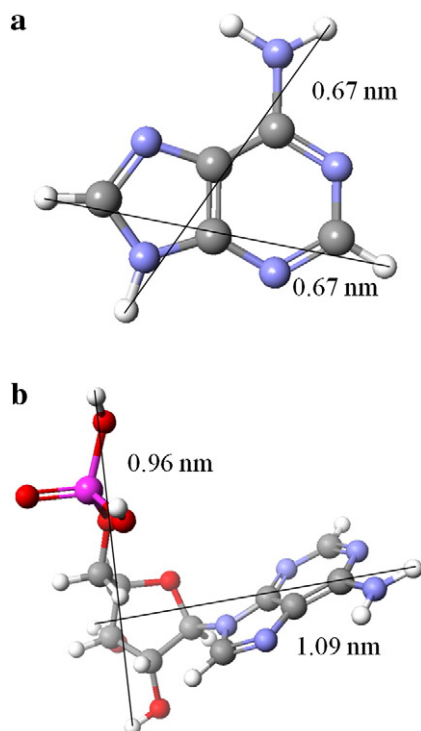
**Table 2**

The adsorption parameters of allophanes calculated from the Freundlich equation.

Adsorbates	Adsorbents	$K_f$ , mmol/g mmol/L <sup>-1/N</sup>	N	$r^{2a}$
Adenine	NP76	0.05	1.1	0.96*
	H <sub>2</sub> O <sub>2</sub> NP76	0.06	1.1	0.90
5'-AMP	NP76	0.18	1.3	0.98
	100 Si/Al-0.5	0.39	1.2	0.97
	100 Si/Al-0.75	0.31	1.2	0.93
	100 Si/Al-1.0	0.48	1.5	0.96
	Pre-100 Si/Al-.05	0.09	1.0	0.99

<sup>a</sup> The values are calculated by a log–log linear regression.

\* Significant at p=0.05 level.

**Fig. 12.** Molecular dimensions of adsorptvities: (a) adenine; (b) 5'-AMP.

## Acknowledgments

This work was supported in part by the Strategic Research Infrastructure Project of the Ministry of Education, Sports, Science and Technology, Japan and the MEXT “Collaboration with Local Communities” Project (2010–2014). The authors are grateful to Anne Austin of Landcare Research, New Zealand for her editorial help.

## References

- Brigatti, M.F., Galan, E., Theng, B.K.G., 2006. Structures and mineralogy of clay minerals. In: Bergaya, F., Theng, B.K.G., Lagaly, G. (Eds.), *Handbook of Clay Science*. Elsevier, Amsterdam, pp. 19–86.
- Cranston, R.W., Inkley, F.A. Adv. 1957. The determination of pore structures from nitrogen adsorption isotherms. *Catalysis* 9, 143–154.
- Engelhardt, G., 1996. Silicon-29 NMR of solid silicates. In: Grant, D.M., Harris, R.K. (Eds.), *Encyclopedia of Nuclear Magnetic Resonance*. John Wiley & Sons, Chichester.
- Giles, C., MacEwan, T., Nakhwa, S., Smith, D.S., 1960. Studies in adsorption. Part XI. A system of classification of solution adsorption isotherms, and its use in diagnosis of adsorption mechanisms and in measurement of specific surface areas of solids. *Journal of the Chemical Society* 148, 3973–3993.
- Hashizume, H., Theng, B.K.G., 2007. Adenine, adenosine, ribose and 5'-AMP adsorption to allophane. *Clays and Clay Minerals* 55, 599–605.
- Hiradate, S., 2004. Speciation of aluminum in soil environments: application of NMR technique. *Soil Sci. Plant Nutrition* 50, 303–314.
- Hiradate, S., Wada, S.I., 2005. Weathering process of volcanic glass to allophane determined by <sup>27</sup>Al and <sup>29</sup>Si solid-state. *Clays and Clay Minerals* 53, 401–408.
- Lippens, B.C., de Boer, J.H.J., 1965. Studies on pore systems in catalysts: V. The t method. *Catalysis* 4, 319–323.
- Loughnan, F.C., 1969. *Chemical Weathering of the Silicate Minerals*. Elsevier, New York, pp. 32–34.
- Mohanan, J.L., Arachchige, I.U., Brock, S.L., 2005. Porous semiconductor chalcogenide aerogels. *Science* 307, 397–400.
- Ohashi, F., Wada, S.I., Suzuki, M., Maeda, M., Tomura, S., 2002. Synthetic allophane from high-concentration solutions: nanoengineering of the porous solid NMR. *Clay Minerals* 37, 451–456.
- Parfitt, R.L., 1990. Allophane in New Zealand – a review. *Australian Journal of Soil Research* 28, 343–360.
- Sinha, R.S., Yamada, K., Okamoto, M., Ogami, A., Ueda, K., 2003. New poly(lactide)/layered silicate nanocomposites.3. High-performance biodegradable materials. *Chemistry of Materials* 15, 1456–1465.
- Theng, B.K.G., Yuan, G., 2008. Nanoparticles in the soil environment. *Elements* 4, 395–399.
- Theng, B.K.G., Russell, M., Churchman, G.J., Parfitt, R.L., 1982. Surface properties of allophane, halloysite, imogolite. *Clays and Clay Minerals* 30, 143–149.
- Van der Gaast, S.J., Wada, K., Wada, S.I., Kakuto, Y., 1985. Small-angle X-ray powder diffraction, morphology, and structure of allophane and imogolite. *Clays and Clay Minerals* 33, 237–243.
- WHO, 2007. The international decade for action: water for life-2005–2015. [http://www.who.int/water\\_sanitation\\_health/wwd7\\_water\\_scarcity\\_final\\_rev\\_1.pdf](http://www.who.int/water_sanitation_health/wwd7_water_scarcity_final_rev_1.pdf)2007 (accessed on 27 October 2011).
- Yuan, G., Wada, S.I., 2012. Allophane and imogolite nanoparticles in soil and their environmental applications. In: Barnard, A.S., Guo, H.B. (Eds.), *Nature's Nanostructures*. Pan Stanford Publishing Pte Ltd, pp. 485–508.